

## Depth-profiling plasma-induced densification of porous low- $k$ thin films using positronium annihilation lifetime spectroscopy

Jia-Ning Sun, David W. Gidley, Yifan Hu, and William E. Frieze  
*Department of Physics, University of Michigan, Ann Arbor, Michigan 48109*

E. Todd Ryan

*Advanced Micro Devices, AMD/Motorola Alliance, Austin, Texas 78721*

(Received 27 February 2002; accepted for publication 21 June 2002)

Positronium annihilation lifetime spectroscopy (PALS) has been used to depth profile the densification induced in a porous low-dielectric constant ( $k$ ) thin film by typical device integration processing, including exposure to plasmas and oxygen ashing. Such “integration damage” has previously been observed as an undesirable increase in  $k$  accompanied by shrinkage in the porous film thickness. PALS confirms that the structural damage is confined to a surface layer of collapsed pores with the underlying pores being undamaged. The dense layer thickness determined by PALS increases with plasma exposure time. © 2002 American Institute of Physics.

[DOI: 10.1063/1.1501767]

There have been extensive efforts to develop ultralow-dielectric constant thin films ( $k$  less than 2.2) as interlayer dielectrics (ILD) to reduce the resistance–capacitance delay in integrated circuits as the microelectronics industry targets<sup>1</sup> minimum device dimensions below 0.10  $\mu\text{m}$ . Engineering *nanoporosity* (introducing pores at the 1–10 nm level) into an insulator has become the dominant strategy to generate the much-needed ultralow- $k$  materials.<sup>2</sup> However, the presence of accessible (possibly interconnected) pores generates problems in porous film device integration since the pores will be exposed to reactive plasmas in typical capping, etching, and ashing processes. Ryan *et al.*<sup>3</sup> recently reported unacceptable increases in  $k$  accompanied with shrinkage of the low- $k$  film after plasma exposure. Detecting degradation of electrical properties after integration is straightforward, but revealing the depth-dependent changes in the tiny pores has few applicable techniques.<sup>4</sup> In this letter, we use depth-profiled positronium annihilation lifetime spectroscopy (PALS), a probe of nanoporous structure in thin films,<sup>5–7</sup> to directly determine the effect of plasma and oxygen ashing exposure on pore morphology. Understanding the fundamental structural effects will not only facilitate prevention of integration damage, but may also permit controlled porosity modification for advanced diffusion barrier development on low- $k$  films.

In using PALS with thin films, a focused monoenergetic beam of positrons is implanted and forms positronium [(Ps) the electron–positron bound state] in the material.<sup>5,6</sup> Ps inherently localizes in the pores where its natural lifetime of 140 ns is reduced by annihilation with molecular electrons during collisions with the pore surfaces. The collisionally reduced lifetime is correlated with void size<sup>5,6</sup> and forms the physical basis for probing pore structure with PALS. The major advantage of depth-profiled PALS is the ability to control the depth distribution of Ps formation by varying the positron beam energy. This is the critical feature that allows analysis of surfaces and the depth-dependent inhomogeneity of the plasma-treated (PT) porous low- $k$  films.

Systematic plasma treatments of an organosilicate, nan-

oporous, methylsilsequioxane (MSQ)-like film were performed to simulate the processing environment that low- $k$  films will encounter during their integration with Cu<sup>3</sup>. The blanket MSQ-like film on a Si wafer has a thickness of 280 nm and porosity of 58%. Three specimens were exposed to a treatment of nitrogen-based plasma in a commercial plasma-enhanced chemical vapor deposition tool at 350 °C for 10 s, 30 s, and 60 s, respectively. A fourth film was treated in a commercial Gasonics asher for 10 s of oxygen plasma ashing.

All these processed films, along with a pair of unprocessed nonporous and porous films as control samples, were depth profiled with PALS by varying the implantation energy from 1 to 8 keV (see Ref. 5 for more details about PALS methodology). For all the porous films, the annihilation lifetime spectrum typically requires at least two long-lived Ps components for acceptable fitting: One component is consistent with Ps annihilating with the vacuum lifetime of  $\sim 140$  ns and the second component of Ps annihilating in the film has an intermediate lifetime  $\leq 45$  ns. The nonporous film has only one long lifetime Ps component, i.e., a small fraction of Ps annihilating in a vacuum as shown in Fig. 1. This is due to backscattered positrons that form Ps at the surface, an ever-present effect when using positron beams. The intensity of backscattered Ps depends inversely upon the implantation energy, as shown in Fig. 1. In the unprocessed porous film, however, much more Ps is detected to annihilate with the vacuum lifetime of 140 ns (Fig. 1), indicating that the pores in this film are highly interconnected and open to the vacuum.<sup>5</sup> With a thermal velocity of  $8 \times 10^6$  cm/s, Ps can diffuse over long distances (on the order of microns) within the interconnected porous network and make tens of thousands of attempts to probe the surface region within its lifetime. Ps can easily escape into the vacuum if its diffusion length is larger than the film thickness. Therefore, a diffusion barrier is required to prevent such escaping of Ps in order to determine the pore size.<sup>5</sup> An 80 nm oxide-capping layer was applied and a single Ps lifetime is fitted to be 45 ns, corresponding to an average cylindrical pore diameter of 2.5 nm.<sup>8</sup>

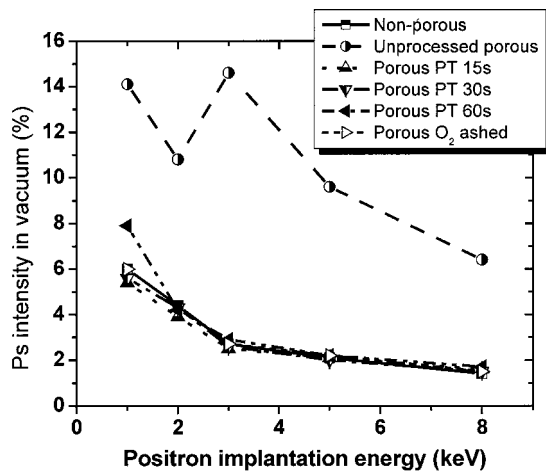


FIG. 1. Ps vacuum intensity in the PT and  $O_2$  ashed films. A pair of unprocessed nonporous and porous films is examined for comparison. The statistical error bars are no larger than the plotting symbols. The lines connecting data points here and in Fig. 2 are simply to guide the eye.

The fitted intensities of Ps in the vacuum of the PT films and the  $O_2$  ashed sample are also plotted in Fig. 1. All these treated films present a similar intensity of Ps in a vacuum as the unprocessed *nonporous* film. This indicates that there is only backscattered Ps in the vacuum and no Ps formed in the film has been able to escape into the vacuum in these processed films. Hence, *the interconnected pores in the porous MSQ-like film are sealed off after the PT or the ashing process*. This *densified, nonporous* layer formed on the surfaces performs effectively as a Ps diffusion barrier. The next question to ask is: How thick is this dense layer and how does the thickness depend on plasma exposure time?

A dense layer suppresses Ps formation in the two long lifetime components, so depth profiling can determine its thickness. For each beam energy, we add the two long-lived Ps intensities and correct for the effect of backscattered Ps by subtracting the respective nonporous film vacuum intensity. This determines the total Ps formed in the mesopores, which depends on beam implantation energy as shown in Fig. 2. Ps formation in the mesopores is markedly decreased in the processed films. In particular, very little Ps annihilates

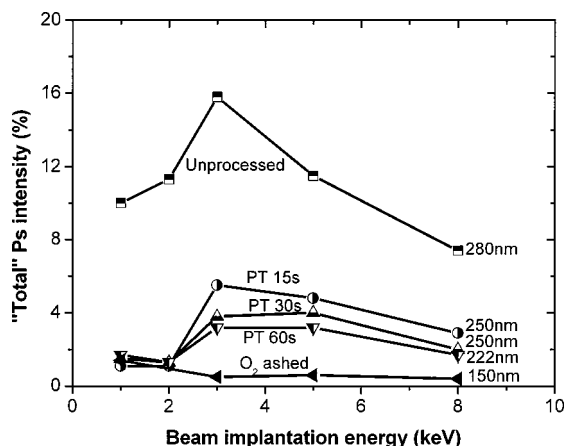


FIG. 2. "Total" Ps formed in mesopores (including Ps diffusing into a vacuum), after correcting for Ps backscattering into the vacuum. Numbers on the right-hand side of the plot are film thicknesses determined using cross-sectional SEM.

in the mesopores at low implantation energies, where most positrons stop close to the surface. At energies of 3 keV and above, more positrons are able to penetrate the dense layer and form Ps in the mesopores underneath. A Ps lifetime around 45 ns is fitted in the mesoporous component, consistent with that observed in the oxide-capped unprocessed film. This indicates that PT processing collapses surface pores *without affecting the porous structure underneath*. The Ps mesoporous intensity starts to decrease at 5 keV in all the films as a result of the deep implantation of positrons into the Si substrate.

Note in Fig. 2 that the Ps mesoporous intensity decreases as the plasma treatment time increases, which means fewer positrons are able to penetrate the densified layer at each implantation energy. This indicates that the densified layer grows deeper into the film with longer PT exposure. We have roughly estimated the thicknesses of the densified layers by making a comparison between the processed films and the unprocessed porous film. For simplicity, we assume that the dense layer is simply formed as a result of the pore collapse and the underneath pore structure has not been affected. Since the positron implantation profile is a function of the product of film density and thickness, the only positron population that accounts for the reduction in the Ps intensity in mesopores of the processed films (compared to the unprocessed film), is that fraction that stops in the dense skin layer. Assuming the Ps mesoporous intensity is proportional to the thickness of the mesoporous layer, we can then estimate the thickness of the remaining mesoporous layer by comparing the Ps intensity values in the processed film with that of the unprocessed film. The average results for each densified layer is then determined to be  $73 \pm 5$  nm,  $84 \pm 7$  nm, and  $90 \pm 5$  nm, respectively for the three nitrogen-based PT films. Despite the fact that the real skin layer thickness can be different depending on the composition of the top layer and the distribution of Ps, these values can give us an idea of how damaging the integration process can be to the porous low- $k$  films. The ashed film, in particular, shows only negligible Ps signal from the mesopores (less than 0.5%) throughout the probed energy range of 1 to 8 keV. It appears that almost all the mesopores have collapsed.

Complementary experiments using a Hitachi 5000 H scanning electron microscope (SEM) have been carried out on these films.<sup>3</sup> The overall thicknesses of the MSQ-like films are measured in cross-sectional SEM images and are presented along the right-hand side edge of Fig. 2. The original thickness of 280 nm shrank to 220 nm after nitrogen-based plasma exposure of 60 s. The film is further thinned to 150 nm in the  $O_2$  ashed film, almost the thickness of the dense analog without any mesopores. This clear evidence of film thinning from SEM analysis strongly favors the pore collapse densification mechanism. The SEM images provide a hint of a densified surface layer (see Fig. 3), but one can not be definitive about how much residual porosity remains, nor can one know if the remaining pores are undamaged. The SEM results are consistent with the hypothesis based on PALS results that a densified layer is formed on top of the porous low-dielectric constant thin film after plasma treatment or ashing process, with the sacrifice of the mesoporosity.

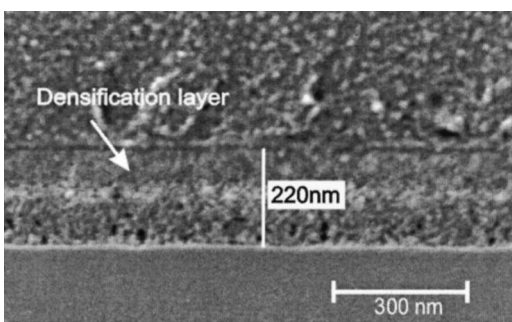


FIG. 3. Cross-sectional SEM image of the nitrogen-based PT 60 s film. A Mbond epoxy layer was deposited on top of the film to facilitate sample preparation.

These results show that a short-time exposure to plasmas can alter the porous structure in low- $k$  films drastically, which will compromise the electrical properties. Electrical testing on these films has demonstrated<sup>3</sup> an increase in the dielectric constant  $k$ , of, for instance, 2.2 to 4 after 60 s of plasma treatment. Clearly, such a large increase in  $k$  as a result of integration processing can not be tolerated and may even exclude such a film as candidates for future ILD applications.

In summary, depth-profiled PALS has been demonstrated to be a simple and powerful technique in probing integration damage in a porous MSQ-like film with highly interconnected porosity. The presence of a densified surface layer induced in the plasma treatment and ashing process is detected as no Ps leakage signal into the vacuum is observed in all of the treated films. Depth-profiling results indicate that this layer grows deeper into the highly interconnected porosity as the nitrogen-based plasma exposure time becomes longer, without changing the sizes of mesopores underneath. The work further demonstrates the unique capability of PALS for detecting the pore structure evolution underneath a dense layer. These overlayers tend to behave as Ps diffusion

barriers. Indeed, the *controlled* development of a very thin “skin” layer, might be a great advantage in preventing Cu diffusion into the underlying dielectrics. It has been reported that the formation of a densified nitride layer on top of hydrogen silsesquioxane film through plasma treatment can suppress Cu diffusion.<sup>9,10</sup> It may be possible to form a dense, continuous skin layer that can effectively barrier the rest of the film from plasma damage. Ideally, this skin layer would perform as the Cu diffusion barrier. More likely, it would be the flat “platform” on which to deposit an ultrathin diffusion barrier. Future work might achieve this through the control of the plasma parameters, exposure time, and the low- $k$  film composition.

The authors acknowledge many helpful discussions with our colleague Dr. Albert Yee at the Institute of Materials Research & Engineering in Singapore. This work is supported by the National Science Foundation (ECS-0100009) and the Low- $K$  Dielectric Program at International Sematech.

<sup>1</sup>Semiconductor Industry Association, *International Technology Roadmaps of Semiconductors* (1999).

<sup>2</sup>B. Zhao and M. Brongo, *Mater. Res. Soc. Symp. Proc.* **565**, 137 (1999).

<sup>3</sup>E. T. Ryan, J. Martin, K. Junker, J. Wetzel, D. W. Gidley, and J. N. Sun, *J. Mater. Res.* **16**, 3335 (2001).

<sup>4</sup>M. Morgan, E. T. Ryan, J.-H. Zhao, C. Hu, T. Cho, and P. S. Ho, *Annu. Rev. Mater. Sci.* **30**, 645 (2000).

<sup>5</sup>D. W. Gidley, W. E. Frieze, A. F. Yee, T. L. Dull, H.-M. Ho, and E. T. Ryan, *Phys. Rev. B* **60**, R5157 (1999).

<sup>6</sup>D. W. Gidley, W. E. Frieze, T. L. Dull, J. N. Sun, A. F. Yee, C. V. Nguyen, and D. Y. Yoon, *Appl. Phys. Lett.* **76**, 1282 (2000).

<sup>7</sup>M. P. Petkov, M. H. Weber, K. G. Lynn, and K. P. Rodbell, *Appl. Phys. Lett.* **77**, 2470 (2000).

<sup>8</sup>T. L. Dull, W. E. Frieze, D. W. Gidley, J. N. Sun, and A. F. Yee, *J. Phys. Chem. B* **105**, 4657 (2001).

<sup>9</sup>P. T. Liu, T. C. Chang, Y. L. Yang, Y. F. Cheng, F. Y. Shin, J. K. Lee, E. Tsai, and S. M. Sze, *Jpn. J. Appl. Phys., Part 1* **38**, 6247 (1999).

<sup>10</sup>K. M. Chang, I. C. Deng, S. J. Yeh, and Y. P. Tsai, *Electrochem. Solid State* **2**, 634 (2000).